

Working temperature calculation of single-core cable by nonlinear finite element method

XIAOKAI MENG¹, PEIJIE HAN², YONGXIN LIU¹, ZHUMAO LU¹, TAO JIN¹

¹State Grid Shanxi Electric Power Research Institute
Shanxi, China

²State Grid Shanxi Electric Power Corporation
Shanxi, China
e-mail: mengxiaokai870618@163.com

(Received: 04.12.2018, revised: 17.04.2019)

Abstract: By simulating the actual working conditions of a cable, the temperature variation rule of different measuring points under different load currents was analyzed. On this basis, a three-dimensional finite element model (FEM) was established, and the difference and influence factors between the simulation temperature and the experimental measured value were discussed, then the influence of thermal conductivity on the operating temperature of the conductor layer was studied. Finally, combined with the steady-state thermal conductivity model and the experimental measured data, the relation between thermal conductivity and load current was obtained.

Key words: cable, finite element simulation model, thermal conductivity, operating temperature

1. Introduction

According to IEC 60216.3-2006, the deterioration degree of cable insulation material can be assessed by the elongation at break (EAB) amounted to 50% of the initial value [1–4], and the lifetime of insulation material is deduced using the Arrhenius model, which is expressed as follows:

$$\lg \tau = E_a / RT + B, \quad (1)$$

where τ is the service lifetime of cable insulation materials (*year*), E_a is the activation energy (kJ/mol), B is the constant related to material property; R is the molar gas constant (8.314 J/mol·K), T is the core temperature (K) and the unit is in absolute temperature.



When Formula (1) is used to extrapolate insulating material life, the working temperature is one of the important factors affecting the accuracy of extrapolation life value. How to acquire accurate cable working temperature has the vital significance for the accurate prediction of the cable insulation material life and the safe operation of the cable, which has also been attracting close attention from the international community.

At present, the calculation of cable working temperature is basically based on IEC-60287, a numerical analytical method, optical fiber measurement temperature and infrared thermometry [5]. Reference 6 gives a discussion of the IEC calculation vs. FEM simulation for various cable line layout, the result indicates that the FEM shows a stronger electromagnetic and thermal interference than predicted by the IEC 60287 standard [6]. A new method of an optimized IEC method to calculate the thermal resistance of air inside ducts was proposed, and it was in good agreement with experiments as well as FEM simulations for a wide range of duct and cable sizes [7]. The advantage of the FEM is that it is adaptable to irregular regions and can adapt to complex material properties and boundary conditions. A boundary element method usually sets infinity truncation area as boundary, and the boundary temperature is equal to the ambient temperature, but the calculated amount of nodes is large when dealing with multi-layer soil or multi-cable laying [8–11].

In this article, step currents were applied to a power cable at the actual working conditions in order to get the temperature variation rules, at first. Secondly, a three-dimensional FEM was established, and the errors between simulation and experimental results were comparatively analyzed. Then the simulation had been conducted to find out the relations between the core temperature and the thermal conductivity of the insulation layer and sheath layer. Finally, the mathematical relationships between the cable core temperature and thermal conductivity were revised, relied on the experimental results and validated under high current.

2. System design and result analysis

2.1. System design

In order to accurately analyze the variation rule of working temperature with the load current and ambient temperature, a temperature measurement system of a cable was set up according to mimic daily working conditions of the cable.

The schematic diagram of the measuring device and distribution of measurement points are shown in Fig. 1. The cable length of EB and CD is three meters, BD is two meters. The distance from measurement point 2 to point 3 is one and a half meters, and measurement point 1 to point 3 is two meters. GQ-AD3000 is a kind of high performance DC power supply, which cannot only steady the output voltage and current but also can provide a maximum current of 300 A. During the experiment, it was used to provide step currents to the cable.

When electricity is applied to a cable, heat is transferred from the conductor to the environment, and the heat at the bottom shifts upward in the process of transfer. Therefore, the top of the cable was selected as the actual temperature measurement layer, in this paper. Several temperature sensors (the margin of error is $\pm 0.1^\circ\text{C}$ and the resolution is 0.01°C) were installed in the cable and the ambient temperature sensor was placed two centimeters from the surface of the cable sheath, as shown in Fig. 2.

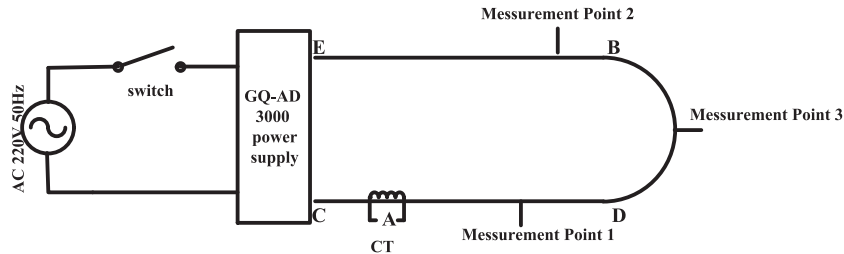


Fig. 1. Schematic diagram of the measuring device

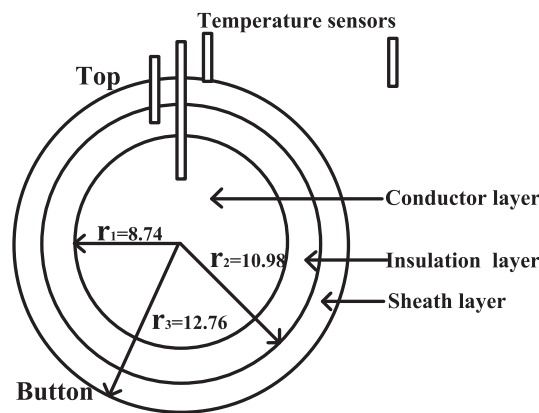


Fig. 2. Schematic diagram of sensors and cross-section of the cable

In order to observe the change trend of the working temperature in different currents, load currents of 50 A, 100 A, 140 A and 200 A were selected in the experiment. The cable was loaded with 50 A at first, and when the core temperature became steady altering less than 1°C in 1 h and the step load current increased to 100 A, then we proceeded to the next load.

2.2. Result analysis

Fig. 3 shows the temperature curves at different measurement points with step currents and it is observed that the core temperature, insulation temperature and surface temperature of each point have the same change trend. With the increase of loading time, the temperature curves increase in terms of logarithm, and as the current increases, the cable temperature needs to take more time to reach a steady state. For example, with a load current of 50 A the core temperature needs about 4 hours to reach a steady state, and when it is of 200 A the core temperature takes about 10 hours to reach this steady state. The increase of the load current also causes the increase of the temperature difference between different layers. The reason of this phenomenon is that the sustained increase of a load current causes more heat in a conductor, but the heat cannot be sent out through the insulation and sheath layer, which also results in the increase of the temperature difference and time to reach a steady state.

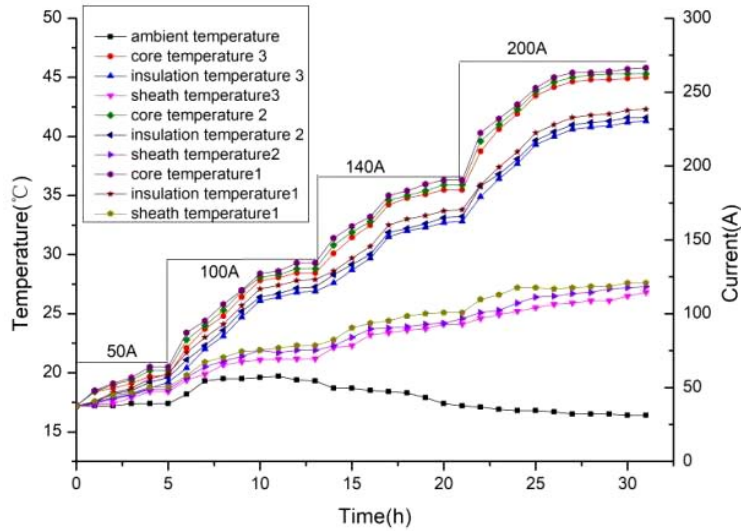


Fig. 3. Temperature curves at different measurement points

Fig. 4 shows the difference of core temperatures among three measurement points. It can be seen that the temperature of measurement point 1 is higher than measurement point 2 and point 3, as well as the temperature differences at 6 h, 9 h, 14 h and 22 h are larger than others. Each of them, except the one at 9 h, appeared after the change of the current and the temperature difference also gradually increased with the current enhancement. For 9 h, the environmental temperature increased from 5 h to 12 h, the efficiency of convection and radiation between the cable skin and environment are decreased and the heat produced by the conductor cannot spread out in time.

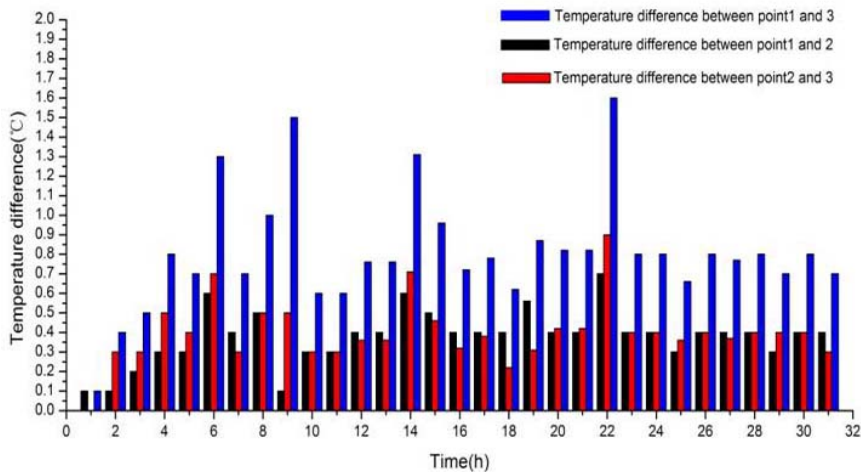


Fig. 4. Core temperature differences of cable in axial

Besides, when load current increases, the contact resistance between the terminal of a cable and power supply will generate more heat, a part of heat will transmit from terminal stud to the core. Since points 1 and 2 were closer to the terminal stud, the temperature of point 1 was higher than point 3 and point 2 in the moment of load current mutation. But after a period of time, the temperatures of the cable core rose and reached a stable state, the temperature differences became smaller. The maximum core temperature difference between measurement point 1 and point 3 was 1.6°C when a current of 200 A was applied.

From the above discussion, in order to reduce the effects of contact resistance, the measurement values of point 3 were selected as the representative of the cable. Because the cable temperature is not easy to be measured directly in actual operation, it can only be deduced by measuring the sheath temperature, load current and environmental temperature. Therefore, in order to accurately analyze the variation of the cable temperature when a load current and ambient temperature change, the temperatures of the surface and environment are used as initial and boundary conditions to establish the FEM.

3. Finite element model analysis

3.1. Geometric modeling

The FEM analysis of a three dimensional convection diffusion equation was given by using an 8-node hexahedral element. The boundary condition was set as the adjacent model, that is, the area around the cable with a radius of 50 mm was used for the analysis, the ambient temperature was taken as the boundary condition of the simulation model as has been shown in Fig. 5, and the model parameters have been shown in Table 1.

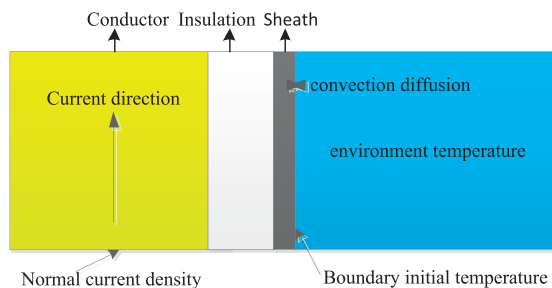


Fig. 5. Boundary condition of FEM

Table 1. Basic parameters of FEM

Parameter	Conductor	Insulation	Sheath	Environment
Material	Copper	EPR	Neoprene	Air
Thickness (mm)	8.74	2.24	1.78	50
Thermal conductivity (W/m·K)	386.4	0.4	0.42	0.023
Specific heat capacity (J/kg·K)	385	221.2	190	–
Density (kg/m ³)	8890	1150	1240	–
Resistivity ($\Omega \cdot \text{m}$)	$1.7241 \text{e}-8$	–	–	–

3.2. Mesh generation

When the cable model was divided into finite element meshes, while all the meshes were small, the calculation turned out to be very time-consuming, and the calculation could not be carried out due to non-convergence. Therefore, two kinds of mesh divided methods were used comprehensively in the analysis process in this paper. For example, because of the characteristics of the cable, its small structure and large temperature gradient, the cable layer was divided by the use of a fine-mesh land model with a grid length of 0.5 mm, which helped to achieve high calculation accuracy. The environment layer was a non-linear aerodynamics model and the change of the temperature gradient was small, so it was just divided by the use of a coarse-mesh scale and the grid length was 2 mm. It is shown in Fig. 6.

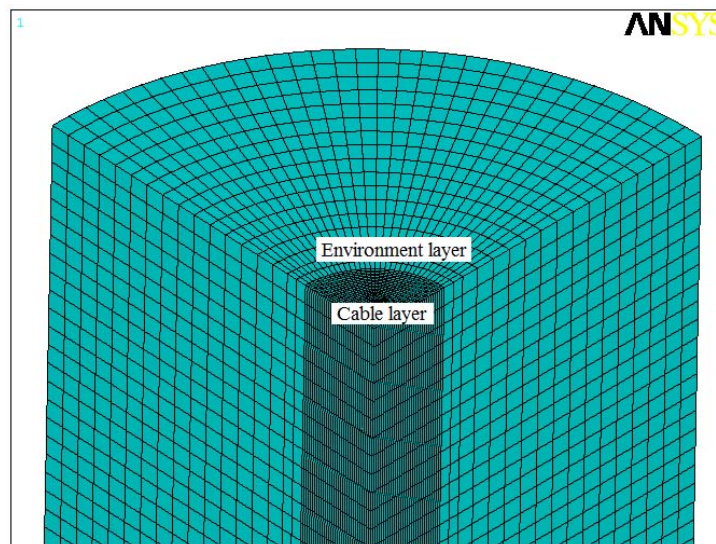


Fig. 6. Diagram of finite element mesh generation

3.3. Simulation results analysis

In the simulation process, there was no external heat sources and the structural parameters of the cable were fixed as shown in Table 1 and were brought into the simulation model in order to analyze the effect of influence factor on the core temperature. The simulation results are obtained when the cable working temperature reaches steady state under a different load current and ambient temperature as shown in Fig. 7.

The steady-state temperature values of the conductor, insulation layer and jacket layer in Fig. 7 were compared with these in Fig. 3, when measurement point 3 of a different load current reaches steady state, the results were shown in Table 2.

According to Table 2, when the load current is 50 A, the difference between the simulation temperature and the experimental data is small. But when the load current increases, the temperature of the conductor, insulation layer and sheath layer is higher than that of the experimental measurement. On the basis of the heat transfer theory and the governing equation of boundary

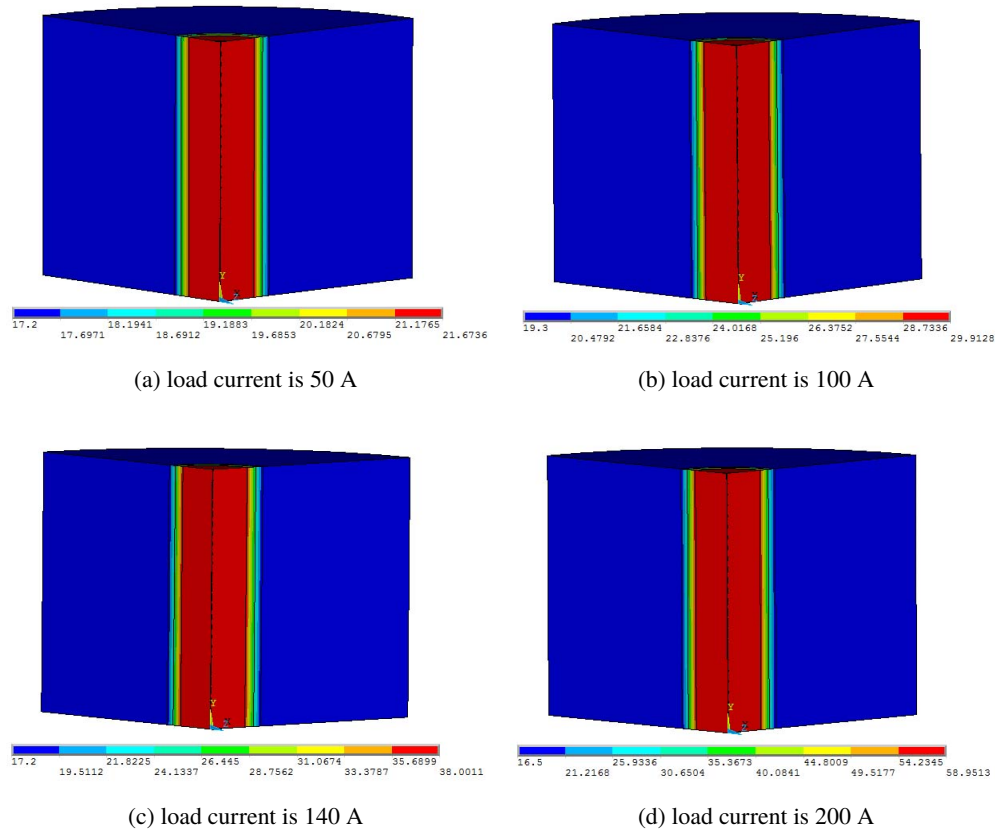


Fig. 7. The steady state simulation values under different load currents

Table 2. Comparison of temperatures of simulation and experiment

		50 A	100 A	140 A	200 A
Simulation temperature (°C)	conductor	21.6	29.9	38.0	58.9
	insulation	21.1	28.7	35.6	54.2
	sheath	18.6	22.8	24.1	30.6
Experiment temperature (°C)	conductor	21.1	28.4	35.4	45.1
	insulation	19.4	26.9	32.7	41.3
	sheath	18.4	21.1	23.7	26.8

conditions, the influencing factors of cable operating temperature mainly include structural parameters, thermal conductivity, an external heat source and environmental temperature. During the simulation process, the cable structure parameters were fixed, there was no influence of the

external heat source, and the ambient temperature was taken into the simulation model as a known boundary condition, therefore, only the influence of the change of thermal conductivity needs to be considered.

In the simulation process, the thermal conductivity of the insulation layer and the sheath layer remained unchanged, which led to the case, where the heat generated by the insulation layer couldn't be transferred to the sheath layer according to the actual situation, resulting in the temperature of the conductor layer and the insulation layer much higher than the experimentally measured value. Therefore, in order to obtain a more accurate simulation model, it is necessary to analyze the change rule of thermal conductivity of an insulation layer and sheath layer under different load currents.

3.4. Thermal conductivity analysis

In order to analyze the influence of thermal conductivity of an insulation layer and sheath layer on the temperature of a cable conductor layer, the steady-state temperature variation rule of the conductor layer, when the thermal conductivity of the insulation layer and sheath layer increased by 10%, 20%, 30% and 40%, was carried out as shown in Table 3.

Table 3. Effect of the thermal conductivity on conductor temperatures

T (°C)		I (A)			
		50	100	140	200
Insulation	10%	21.4	29.3	37.2	56.6
	20%	21.2	28.8	36	54.6
	30%	21	28.4	35.4	52.9
	40%	20.9	28.0	34	51.5
Sheath	10%	21.5	29.8	37.8	57.4
	20%	21.3	29.2	37.1	56.7
	30%	21.2	28.7	36.5	56.1
	40%	21.1	28.5	35.9	55.6

Fig. 8 and Fig. 9 show the effect of thermal conductivity of insulation and sheath layers on conductor temperature. It can be noted that:

- the higher the load current, the greater the effect of the thermal conductivity on the conductor temperature,
- at the same time, the thermal conductivity of the insulation layer has greater influence on the conductor temperature than that of the sheath layer.

Therefore, in order to obtain the change rule of thermal conductivity with temperature under different load currents, the thermal conductivity of the insulation and sheath layers was assumed to be a one-dimensional steady-state heat conduction problem along the radius [12, 13], as shown in Fig. 10. There, the radius of the conductor, insulation and sheath layers were r_c , r_1 ,

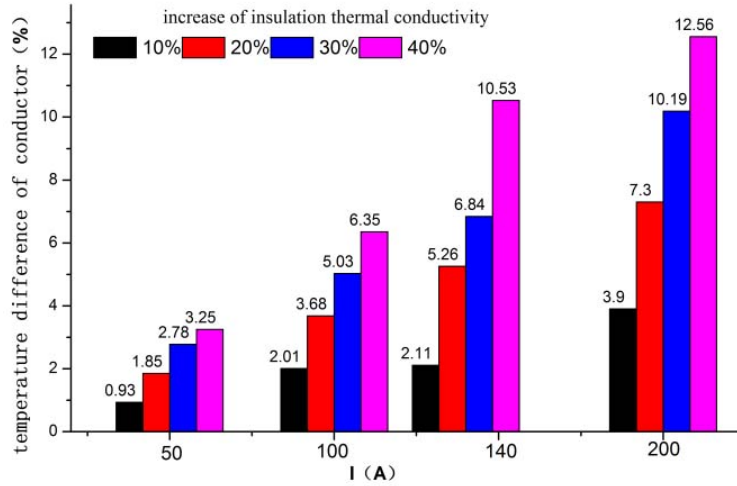


Fig. 8. Effect of thermal conductivity of insulation on conductor temperature

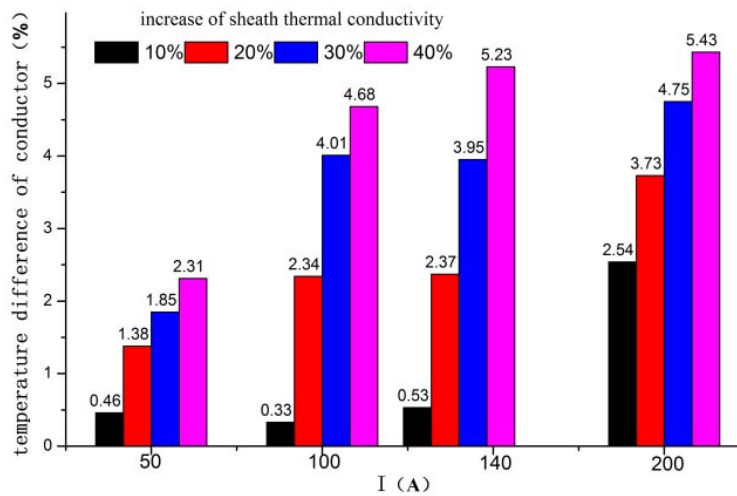


Fig. 9. Effect of thermal conductivity of sheath on conductor temperature

r_2 , respectively. T_1 was the inner surface temperature of the insulation layer, T_2 was the external surface temperature.

According to the heat conduction theory, the differential equation of heat conduction at any point of the insulation layer is:

$$\frac{d}{dr} \left(r \frac{d\theta}{dr} \right) = 0. \tag{2}$$

The boundary condition is $r = r_c : T = T_1, r = r_1 : T = T_2$.

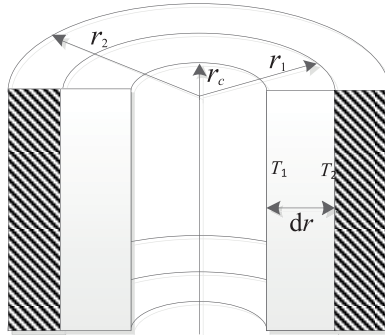


Fig. 10. Steady-state heat conduction model of insulation layer

Integrating Function (2) and conjunction with boundary conditions yields:

$$C_1 = \frac{T_2 - T_1}{\ln(r_1/r_c)}, \quad C_2 = T_1 - \frac{T_2 - T_1}{\ln(r_1/r_c)} \ln r_c. \quad (3)$$

The temperature of the insulation at any point is:

$$T = T_1 + \frac{T_2 - T_1}{\ln(r_1/r_c)} \ln \frac{r}{r_1}. \quad (4)$$

Take the logarithm of both sides, and the heat flux q of the insulation layer obtained by Fourier's law is:

$$q = \frac{\lambda}{r_c} \frac{T_2 - T_1}{\ln(r_1/r_c)}. \quad (5)$$

The total heat flux W_d through the insulation layer of unit length is:

$$W_d = \frac{2\pi\lambda(T_2 - T_1)}{\ln(r_1/r_c)}. \quad (6)$$

The thermal resistance T_d of the insulation layer is:

$$T_d = \frac{\ln(r_1/r_c)}{2\pi\lambda}. \quad (7)$$

So, the insulation layer temperature difference between θ_2 and θ_1 can be expressed as:

$$T_2 - T_1 = (I^2R + 0.5W)T_d, \quad (8)$$

where: W is the insulation loss, $W = U_0^2 \omega C \tan \delta$, U_0 is the insulation voltage, ω is the angle frequency, $\tan \delta$ is the dielectric loss tangent, C is the capacitance per unit length.

Therefore, the thermal conductivity λ of the insulation layer is:

$$\lambda = \frac{I^2R + 0.5U_0^2\omega C \tan \delta}{2\pi(T_2 - T_1)} \ln(r_1/r_c), \quad (9)$$

where: I is the load current, R is the AC resistance per unit length.

First, the thermal conductivity of the insulation layer was calculated by bringing the temperature values on both sides of the insulation layer under different loads into Equation (9). Then, the results and load currents were taken into the simulation model and corrected the thermal conductivity of the insulation and sheath layer by using the experimental temperature data. The simulation results are shown in Table 4.

Table 4. Computing results of temperature and thermal conductivity

		50 A	100 A	140 A	200 A
Simulation temperature (°C)	conductor	21.6	28.8	35.3	46.5
	insulation	21.1	27.7	33.3	42.3
	sheath	18.6	22.4	23.2	26.2
Experiment temperature (°C)	conductor	21.1	28.4	35.4	45.1
	insulation	19.4	26.9	32.7	41.3
	sheath	18.4	21.1	23.7	26.8
Thermal conductivity	insulation	0.4	0.48	0.54	0.64
	sheath	0.42	0.44	0.46	0.5

The thermal conductivity could only be estimated according to the cable temperatures and load current, but could not be calculated by using the cable temperature distribution as the temperature of the conductor, and the insulation layer could not be measured directly under normal operating conditions. According to the above analysis, the temperature of the cable conductor layer was mainly determined by the load current and the thermal conductivity of the insulation layer and sheath layer. On the other hand, the fundamental factor that affected the change of the thermal conductivity of the conductor temperature, insulation layer and jacket layer was the load current.

In order to get the thermal conductivity at other load currents, the equations were obtained by fitting the curve of the thermal conductivity to the load current, as shown in Fig. 11.

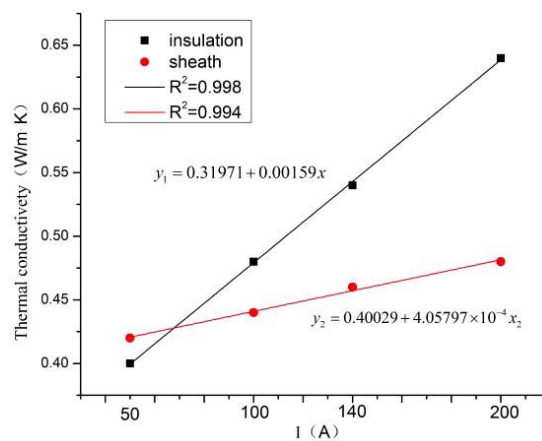


Fig. 11. The relationship between thermal conductivity and current

In order to verify the accuracy of the relationship between the thermal conductivity and load current of the insulation layer and sheath layer, the load current was set at 250 A under the experimental conditions, and the temperature value of each layer of the cable and the environmental temperature value of measuring point 3 were recorded. The simulation results are shown in Fig. 12 and Fig. 13.

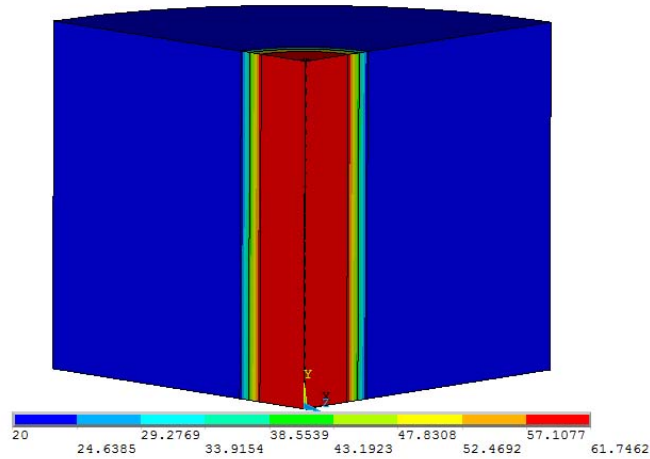


Fig. 12. The steady state simulation result of 250 A

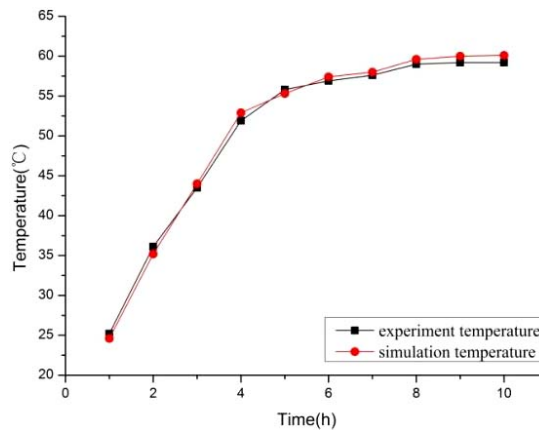


Fig. 13. The contrast curve of experiment and simulation result

4. Conclusion

The temperature measurement system was constructed by simulating the actual working conditions of the cable and the temperature of different measuring points under different load currents was obtained. Then, the error and influence factors of the temperatures during the

experimental tests were measured and the FEM under the fixed condition of the cable parameters were analyzed. In addition, the relationship between the thermal conductivity and the load current was studied by combining the steady-state thermal conductivity model with the experimental measured data. The proposed method has the following advantages:

1. When the cable parameters are fixed, there is a large deviation between the simulated temperature and the experimental measured value, and it increases with the increase of the load current.
2. The steady-state temperature change law of a conductor layer was analyzed when the thermal conductivity of an insulation layer and sheath layer was increased by 10%, 20%, 30% and 40%, the results show that the influence of the thermal conductivity of an insulation layer on the temperature of a conductor layer was greater than that of a sheath layer.
3. The relationship between thermal conductivity and load current was obtained by combining the steady-state thermal conductivity model and the experimental measurement temperature, and the measurement value of the load current was taken as 250 A for verification. The results showed that the error between the simulated temperature value and the experimental measurement value was small.

References

- [1] Simmons K.L., Fifield L.S. *et al.*, *Determining remaining useful life of aging cables in nuclear power plants-interim study FY13*, Pacific Northwest National Laboratory, pp. 1–5 (2013).
- [2] Hexun W., Yu-long J. *et al.*, *Accelerated aging experiment and remaining lifetime analysis of insulation for CXF type cable on vessels*, High Voltage Engineering, vol. 39, no. 8, pp. 1886–1992 (2013).
- [3] Risch B.G., Bowman R.E., *Cable material reliability for industrial and harsh environment applications*, International Wire and Cable Symposium: Proceedings of the 61st IWCS conference, pp. 533–542 (2012).
- [4] Zhiqiang W., Changliang Z., Wenwen L., Guofeng L., *Residual life assessment of butyl Rubber insulated cables in shipboard*, Proceedings of the CSEE, vol. 32, no. 8, pp. 189–195 (2012).
- [5] Hwang C.-C., Jiang Y.-H., *Extensions to the finite element method for thermal analysis of underground cable system*, Electric Power Systems Research, vol. 64, no. 2, pp. 159–164 (2003).
- [6] Stefanis Conti, Emanuele Diletto, Santi Agation Rizzo, *Electromagnetic and thermal analysis of high voltage three-phase underground cable using finite element method*, 2018 IEEE International Conference on Environment and Electrical Engineering and 2018 IEEE Industrial and Commercial Power Systems Europe, pp. 1–6 (2018).
- [7] Ali Sedaghat, Haowei Lu, Abdullah Bokhari, *Enhanced thermal model of power cables installed in ducts for ampacity calculations*, IEEE transaction on power delivery, vol. 33, no. 5, pp. 2404–2411 (2018).
- [8] Lili Gu, Xiong Chen, Shijing Zhu, *Study on ampacity calculation of cable in the tunnel based on finite element method*, Advances in intelligent systems research, International conference on mathematics, modeling, simulation and algorithms, pp. 340–344 (2018).
- [9] Muhatifah Mohd Salleh, Mohd Hafiez Izzwan Saad, Yanuar Z. Arief, *Water tree simulation on underground polymeric cable using finite element method*, Journal of telecommunication, electronic and computer engineering, vol. 10, no. 1, pp. 107–112 (2018).
- [10] Meng X.K., Wang Z.Q., Li G.F., *Dynamic analysis of core temperature of low-voltage power cable based on thermal conductivity*, Canadian Journal of Electrical and Computer Engineering, vol. 39, no. 1, pp. 59–65 (2016).

- [11] Ming L., Gang L., *Real-time core temperature calculation on single-core cable by nonlinear finite element method*, Power System Technology (in Chinese), vol. 11, no. 35, pp. 163–169 (2011).
- [12] Shanming L., Wangqing H., *Theoretical research on temperature field of power cable joint with FEM*, International Conference on System Science and Engineering, pp. 564–568 (2012).
- [13] Yongchun L., *Steady-state thermal analysis of power cable systems in ducts using streamline upwind/Petrov Galerkin finite element method*, IEEE Transactions on Dielectrics and Electrical Insulation, vol. 19, no. 1, pp. 283–290 (2012).